Materials Today Bio 26 (2024) 101058

Contents lists available at ScienceDirect

Materials Today Bio

journal homepage: www.journals.elsevier.com/materials-today-bio

# High-viscosity driven modulation of biomechanical properties of human mesenchymal stem cells promotes osteogenic lineage

Yin-Quan Chen [a,*], Ming-Chung Wu [b], Ming-Tzo Wei [c], Jean-Cheng Kuo [b], Helen Wenshin Yu [b], Arthur Chiou [d]

[a] Cancer Progression Research Center, National Yang Ming Chiao Tung University, Taipei, Taiwan
[b] Institute of Biochemistry and Molecular Biology, National Yang Ming Chiao Tung University, Taipei, Taiwan
[c] Department of Chemical and Biological Engineering, Princeton University, Princeton, NJ, USA
[d] Institute of Biophotonics, National Yang Ming Chiao Tung University, Taipei, Taiwan

ARTICLE INFO

*Keywords:*
Extracellular fluid viscosity
Osteogenesis
Cell mechanical properties
TRPV4
NFATc
YAP

ABSTRACT

Biomechanical cues could effectively govern cell gene expression to direct the differentiation of specific stem cell lineage. Recently, the medium viscosity has emerged as a significant mechanical stimulator that regulates the cellular mechanical properties and various physiological functions. However, whether the medium viscosity can regulate the mechanical properties of human mesenchymal stem cells (hMSCs) to effectively trigger osteogenic differentiation remains uncertain. The mechanism by which cells sense and respond to changes in medium viscosity, and regulate cell mechanical properties to promote osteogenic lineage, remains elusive. In this study, we demonstrated that hMSCs, cultured in a high-viscosity medium, exhibited larger cell spreading area and higher intracellular tension, correlated with elevated formation of actin stress fibers and focal adhesion maturation. Furthermore, these changes observed in hMSCs were associated with activation of TRPV4 (transient receptor potential vanilloid sub-type 4) channels on the cell membrane. This feedback loop among TRPV4 activation, cell spreading and intracellular tension results in calcium influx, which subsequently promotes the nuclear localization of NFATc1 (nuclear factor of activated T cells 1). Concomitantly, the elevated intracellular tension induced nuclear deformation and promoted the nuclear localization of YAP (YES-associated protein). The concurrent activation of NFATc1 and YAP significantly enhanced alkaline phosphatase (ALP) for pre-osteogenic activity. Taken together, these findings provide a more comprehensive view of how viscosity-induced alterations in biomechanical properties of MSCs impact the expression of osteogenesis-related genes, and ultimately promote osteogenic lineage.

## 1. Introduction

Human Mesenchymal stem cells (hMSCs), capable of self-renewal and differentiation into various cell types, are promising for treating osteoporosis [1,2]. Although hMSCs for osteoporosis treatment has been demonstrated in animal models and preclinical investigations, various challenges have yet to be overcome for their clinical application [3,4]. To date, the pursuit of effective methods to enhance the osteogenic differentiation of MSCs for clinical application in osteoporosis treatment, remains an ongoing active area of research [5–7].

Biomechanical cues in the cell microenvironment have been identified as crucial stimuli that can alter gene expression, reorganize the cytoskeleton, and influence the distribution of focal adhesions, to modulate various physiological functions of cells, including proliferation, migration, and differentiation [8,9]. These biomechanical stimuli include factors such as fluid shear stress, substrate stiffness, geometric patterns, mechanical stretching, and viscosity [10–12]. Previous research has shown that hMSCs, cultured on substrates with a stiffness exceeding 25 kPa, tend to undergo osteogenic differentiation [13]. Rabbit bone marrow-derived MSCs, exposed to oscillatory shear stress at 10 mPa, effectively enhance their osteogenic differentiation [14]. Likewise, hMSCs, cultivated on polydimethylsiloxane (PDMS) membranes and subjected to cyclic stretching via a mechanical stretching device (with 8 % strain and 1 Hz frequency), promote their osteogenic differentiation [15]. Moreover, the guidance provided by cell geometry, specifically through micropatterning with square and circular shapes of

* Corresponding author.
*E-mail address:* ycchen123@nycu.edu.tw (Y.-Q. Chen).

https://doi.org/10.1016/j.mtbio.2024.101058
Received 15 January 2024; Received in revised form 10 April 2024; Accepted 13 April 2024
Available online 16 April 2024

the same area (2883 μm$^2$), significantly influences hMSC differentiation. Square patterns generally favor osteogenic differentiation, while circular patterns tend to induce adipogenic differentiation [16].

Viscosity stands as a crucial property in the realm of biomedical sciences, dictating the flow behavior of fluids, including those inherent to biological systems [17,18]. Within biomedical applications, a comprehensive understanding of viscosity is paramount for numerous processes, encompassing drug delivery [19], tissue engineering [20], and diagnostic methodologies [21]. One notable application of hydrogel viscosity in biomedical engineering emerges in the realm of 3D bioprinting. Hydrogel viscosity serves as a supportive biomaterial, facilitating diverse avenues for biofabrication, particularly evident in extrusion-based bioprinting of bioinks [22]. Furthermore, a recent study from Bera et al. [23] has pinpointed extracellular fluid (ECF) viscosity as a notable biomechanical trigger capable of altering the mechanical characteristics of cancer cells. This alteration can, in turn, enhance the migration and invasion of cancer cells [23]. A highly viscous ECF regulates various mechanical characteristics in cancer cells, including cell adhesion, traction force generation, and migratory capabilities, and jointly promotes cancer metastasis [24]. Additionally, ECF viscosity may serve as a crucial biomechanical cue influencing and regulating the mechanical properties and differentiation capacity of stem cells. The viscosity of the physiological microenvironment of hMSCs, specifically in the bone marrow, ranges from 37.5 to 400 cP, which is significantly higher than that of the culture medium (0.98 cP) [25]. However, it remains uncertain whether hMSCs response to the mechanical environments induced by viscosity can be harnessed to promote osteogenic differentiation. Furthermore, the mechanisms underlying how hMSCs respond to viscosity stimulation, and to ultimately enhance osteogenic differentiation, remain elusive.

TRPV4 (transient receptor potential vanilloid sub-type 4) is a non-selective cation channel that plays a crucial role in sensing shear stress [26,27], mechanical strain [28], and viscosity [23,24]. The translocation of TRPV4 protein from the cytoplasm to the cell membrane is a crucial step in facilitating calcium influx [29,30]. TRPV4 activation, in response to mechanical stimuli, increases calcium influx, and activates the Rho kinase signaling pathway [31], which in turn directs the reorganization of the cytoskeleton and focal adhesions [32]. Furthermore, the cell cytoskeleton and focal adhesions play crucial roles in mechanotransduction, serving as essential components that transmit extracellular stimuli and initiate a signaling cascade [33,34]. This cascade results in various changes in cell mechanical properties, encompassing alterations in cell morphology, viscoelastic properties, adhesion, and traction forces, all of which affect the cell functions [35,36]. The Yes-associated protein (YAP) assumes a pivotal role as a mechanosensitive protein, acting as a vital link between biomechanical stimulation, cellular mechanics, and the physiological and pathological functions of cells [37,38]. The translocation of YAP into the nucleus stands as a critical factor in the promotion of osteogenesis [39], and this translocation is facilitated by biomechanical cues, such as substrate stiffness, cell spreading area, shear stress, and traction force [38,40,41]. Additionally, the deformation of cells' nuclei, due to higher intracellular tension, has been acknowledged as a crucial mechanism in driving YAP nuclear translocation [42–44]. Thus, these cellular mechanical properties can serve as the indicators of the differentiation potential of hMSCs, as well as the critical targets for significant mediators that can be manipulated to enhance hMSCs differentiation [36,45].

In this study, we aimed to explore the potential application of manipulating ECF viscosity to improve the biomechanical characteristics of hMSCs and subsequently promote osteogenic differentiation. Additionally, we sought to understand the role of viscosity stimulation in regulating the process of osteogenesis. Our findings unveiled that high ECF viscosity rapidly enhanced the biomechanical properties of hMSCs, including an increase in cell spreading area and heightened intracellular tension. Furthermore, our findings revealed a noteworthy connection between viscosity-induced alterations in biomechanical properties and the translocation and activation of TRPV4 channels on the cell membrane. This activation subsequently increased calcium influx and raised intracellular tension, which played a role in expanding cell spreading and causing nuclear deformation. These effects, in turn, facilitated the nuclear translocation of both NFATc and YAP, and ultimately enhanced osteogenic lineage.

## 2. Material and method

### 2.1. Cell culture

Human mesenchymal stromal cells (hMSCs) were purchased from Lonza (PT-2501). hMSCs were cultivated in DMEM (low glucose) supplemented with 10 % FBS (SH30070.03, Cytiva Hyclone) and 1 % penicillin/streptomycin (15140-122, Gibco). hMSCs passage ranging from 4 to 7 [42] were used in this study. For osteogenesis induction, we used the osteogenesis induction medium (OIM) composed of 0.1 μM dexamethasone (D8893, Sigma), 5 mM β-glycerophosphate (G9422, Sigma), and 50 μM L-ascorbic-2-phosphate (FL-4972, Sigma). For adipogenesis induction, we used the adipogenesis induction medium (AIM) contains 1 μM dexamethasone (SI-D8893, Sigma), 0.5 mM 3-isobutyl-1--methylxanthine (I5879, Sigma), 10 μg/mL insulin (12585-014, Gibco), and 100 μM indomethacin (I8280, Sigma). In cases of mixed differentiation, we used a 1:1 ratio of OIM and AIM media, fostering a more moderate differentiation environment wherein hMSCs have equal opportunities to enter either osteogenic or adipogenic pathways [46–49].

### 2.2. Staining of MSCs to detect ALP activity and lipid droplets

The effectiveness of directed differentiations was evaluated by using alkaline phosphatase (ALP) staining for osteogenesis and Oil Red O staining for adipogenesis. The procedure for staining hMSCs followed previously established methods [50,51]. Initially, cells were fixed using 4 % paraformaldehyde, followed by a PBS rinse. Subsequently, they were subjected to staining with Fast BCIP/NBT (B1911, Sigma) to identify alkaline phosphatase (ALP) activity. Following this, the cells underwent a 60 % isopropanol rinse and were stained with 30 mg/mL Oil Red O (1320-06-5, Sigma) in 60 % isopropanol to detect lipids. Finally, the cells were stained with 5 μg/mL of Hoechst 33342 (H3570, Thermo Fisher Scientific) for cell counting via a Nikon Eclipse TE100 microscope equipped with a 10 × air objective (MRH00105, Nikon; numerical aperture = 0.3).

### 2.3. Immunofluorescence staining

The primary antibodies used in this experiment were 1:100 dilution of anti-TRPV4 rabbit antibody (65893, Cell Signaling), 1:50 dilution of anti-NFATc1 mouse monoclonal antibody (sc-7294, Santa Cruz Biotechnology), 1:200 dilution of anti-paxillin rabbit polyclonal antibody (GTX125891, GeneTex), and 1:200 dilution of anti-YAP rabbit polyclonal antibody (GTX129151, GeneTex). Stainings via 5 μg/mL of Hoechst 33342 (H3570, Thermo Fisher Scientific) and 165 nM of rhodamine–phalloidin (R415, Thermo Fisher Scientific) were used to visualize cell nuclei and F-actin, respectively. Immunofluorescence images were captured using an epi-fluorescence microscope system (Eclipse Ti, Nikon) equipped with a 40 × oil-immersion objective (MRH01401, Nikon; numerical aperture = 1.3).

### 2.4. Immunostaining for TRPV4 on the cell surface

To identify TRPV4 on the cell membrane, hMSCs were fixed with 4 % paraformaldehyde for 10 min and subsequently rinsed twice with PBS. Then, non-permeabilized fixed MSCs were subjected to a series of 1-h blocking steps with 3 % BSA, followed by a 1-h incubation with anti-TRPV4 antibodies and two subsequent PBS washes; the cells were then exposed to an Alexa Fluor 488-conjugated antibody for 1 h.

### 2.5. Preparation of medium with various viscosities

To modulate the viscosity of the culture medium, we added different concentrations of methylcellulose (M0512, Sigma), an inert viscosity modifying agents, into the cell culture medium at four specific levels (0 %, 0.2 %, 0.4 %, and 0.8 %). The viscosities at these concentrations were subsequently quantified using a rheometer (HR-2, TA Instruments). The osmolarity of 0.8 % MC solution (296.3 ± 3.3 mmol/kg) approached the critical range of normal osmolality of the extracellular fluid (275–295 mmol/kg) (Fig. S5A). This criticality restricted our ability to further increase viscosity levels without compromising the integrity of the cell culture environment.

### 2.6. Interference reflection microscopy

We followed the established procedures for interference reflection microscopy (IRM) with minor adjustments [52,53]. Specifically, an IRM setup was integrated into an epi-fluorescence microscope (Ti Eclipse, Nikon). This setup included a filter cube comprising an excitation filter (535 nm band-pass filter) and a beam splitter (80/20; Reflection/-Transmission). The light reflected from the sample was gathered using a 60× oil-immersion objective (MRD01691, Nikon, numerical aperture = 1.49) and then directed through the 80/20 beam splitter into a CMOS camera (DMK 33UX174, Imaging Source) for image capture. Time-lapse IRM images were imported into ImageJ software, and the cell edges were manually traced to determine the cell area at successive time points.

### 2.7. Traction force microscopy

hMSCs were cultured on polyacrylamide gels (PA) with a stiffness of 21.5 kPa coated with fibronectin. These elastic PA gels were created using a mixture containing acrylamide (1610140, Bio-Rad) and Bis-acrylamide (1610142, Bio-Rad) at final concentrations (v/v) of 10 %/0.2 % [54]. Additionally, 200 nm-diameter fluorescent beads (F8810, Thermofisher) were incorporated into the gel mixture. The displacement of these fluorescent beads around cells with vs. without trypsin treatment were recorded using an epi-fluorescence microscope system (Eclipse Ti, Nikon) equipped with a 60 × oil-immersion objective (MRD71670, Nikon; numerical aperture = 1.49). The analysis of particle displacements was carried out using PIVlab software [55]; and the traction forces and intracellular tension were calculated using the TFMatlab software [56–58].

### 2.8. Calcium imaging

To track the calcium influx in hMSCs, cells were loaded with Fluo-8 AM (ab142773, abcam), a green fluorescent calcium indicator, for visualizing and quantifying intracellular calcium levels. hMSCs were initially incubated in DMEM without additional FBS and penicillin/streptomycin (P/S) for 1 h. Following this, they were exposed to 5 μM of Fluo8-am for 1 h. Finally, the cells were rinsed twice with PBS and placed back into the growth medium. Imaging of intracellular calcium signals was accomplished using an epi-fluorescence microscope (Ti-E, Nikon) equipped with an 60× oil-immersion objective (MRD01691, Nikon, numerical aperture = 1.49) and a CMOS camera (DMK 33UX174, Imaging Source).

### 2.9. Analysis of nuclear volume

To assess the volume and deformation of nuclei, we stained the nuclei with 10 μM of Hoechst 3324 and captured 3D nuclear images with a z-step size of 0.25 μm utilizing a laser scanning confocal microscope system (LSM 900, ZEISS), equipped with a plan-apochromat 63 × oil-immersion objective lens (420782-9900-000, Zeiss, numerical aperture = 1.4). The 3D micrographs of nuclei were obtained via ZEN software (Zeiss). The nuclear morphology, including nuclear volume, maximum projected area, and nuclear thickness, was quantified via the Fiji software.

### 2.10. Image analysis

The assessment of individual focal adhesion (FA) area and the count of FAs per cell were conducted using MetaMorph software. Additionally, ImageJ software was applied to analyze the fluorescence intensity of TRPV4, and NFATc of hMSCs. The N/C ratio was determined by dividing the mean fluorescence intensity of the cell nucleus by that of the cytoplasm.

### 2.11. Statistical analysis

Statistical analysis of the data was conducted using MATLAB; it involved one-way ANOVA, followed by Tukey's test for post hoc analysis. The statistical significance is represented as * for $p < 0.05$, ** for $p < 0.01$, and N.S. (not significant), as indicated in the figures.

## 3. Results

### 3.1. Higher viscosity of extracellular fluid enhanced cell spreading

To examine the impact of ECF viscosity on the biomechanical properties and the differentiation of hMSCs, we modified the viscosity of the culture medium by adding different concentrations of methylcellulose (MC) at four distinct levels (0 %, 0.2 %, 0.4 %, and 0.8 %). The resulting viscosities, measured via a rheometer, revealed a significant increase in medium viscosity as the concentration of MC increased. Specifically, the viscosities of cell culture medium supplemented with the four different MC concentrations (0 %, 0.2 %, 0.4 %, and 0.8 %) were 0.98 ± 0.04, 8.44 ± 1.94, 21.83 ± 3.21, and 68.14 ± 1.59 cP, respectively (Fig. 1A and B). Furthermore, compared to the viscosity of the cell culture medium, the viscosity levels achieved with 0.4 % and 0.8 % MC supplementation more closely resembled the viscosity (37.5–400 cP) of the hMSCs' physiological microenvironment, such as the bone marrow [25].

We then proceeded to assess the impact of medium viscosity on various biomechanical properties, such as cell spreading area, actin polymerization, and focal adhesion formation. In order to gain a comprehensive understanding of how cells adhered and spread in response to viscosity stimulation over time, we cultured hMSCs on a glass-bottom dish and examined them via interference reflection microscopy (IRM). The time-lapse images provided a clear depiction of hMSCs rapidly initiating spreading and protrusion upon exposure to the high-viscosity medium (Fig. 1C and Supplementary Movie 1). Notably, the higher viscosity medium resulted in a significant increase in cell spreading area (Fig. 1D and E). Furthermore, to assess the prolonged effect of viscosity stimulation on cell spreading, we conducted experiments capturing time-lapse images of hMSCs in regular culture medium, as well as in high-viscosity medium (68.14 cP) over a 6-h period (Supplementary Movie 2). Upon the addition of the viscous medium, we immediately observed an increase in the cell spreading area, reaching an initial plateau after approximately 60 min (Fig. S1 A-C). Subsequently, fluctuations in cell spreading area associated with cell retraction and protrusion, indicative of cell migration, were observed beyond the 1-h mark (Fig. S1 A-C).

Supplementary data related to this article can be found online at https://doi.org/10.1016/j.mtbio.2024.101058

### 3.2. Higher viscosity of extracellular fluid enhanced actin stress fibers and focal adhesions formation

Cell morphology and spreading are regulated by the dynamics of the cytoskeleton and focal adhesions [59–61]. Next, we sought to delve into

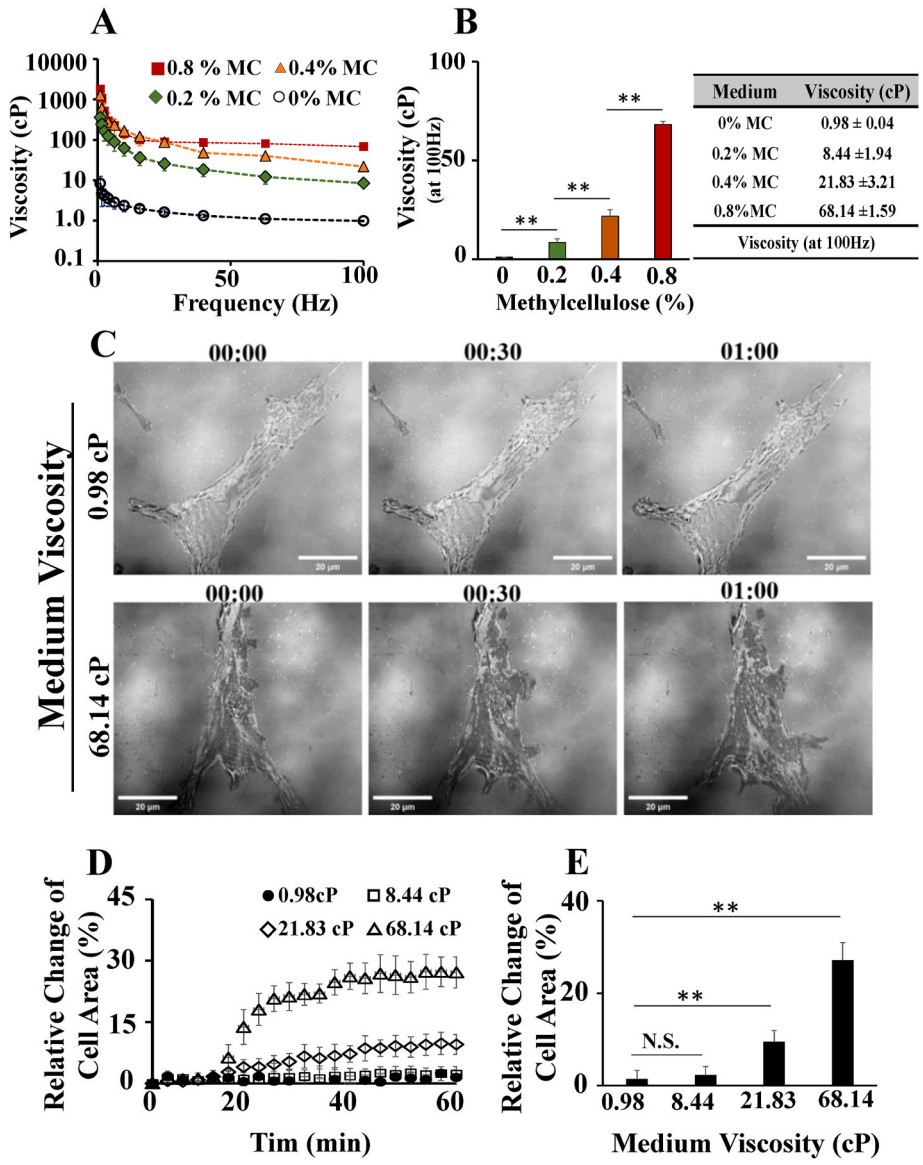


**Fig. 1.** Higher viscosity of extracellular fluid significantly increased the spreading area of human mesenchymal stem cells (hMSCs). (A) Different values of viscosity of the culture medium (DMEM) were obtained by supplementing it with different concentrations (w/v) of methylcellulose (MC) at 0 %, 0.2 %, 0.4 %, and 0.8 %, and measured by a rheometer. All measurements were maintained at 37 °C over the range of 0.05–100 Hz. Data represent mean ± SD (n = 3; i.e., three replicated independent experiments). **(B)** Right: Statistical comparisons were conducted for the viscosity of all viscous media at 100 Hz. Data represent mean ± SD (n = 3; i.e., three replicated independent experiments). Left: The viscosity of each medium measured at a shear rate of 100 Hz and a temperature of 37 °C. **(C)** Interference reflection micrographs of hMSCs were captured at three sampling time points: 0, 30, and 60 min after the culture medium (0.98 cP) was replaced by a high-viscosity medium (68.14 cP). Scale bars = 20 μm. **(D)** The relative change in hMSCs' area over time (t) after a change in the medium with different viscosities. The relative change (%) = {[A(t) - A(0)]/A(0) × 100}, where A(0) and A(t) represent cell area at 0 min and at different time points "t", respectively. Data represent mean ± SD (n = 10). **(E)** The corresponding relative change in cell area over 60 min. Data represent mean ± SD (n = 10). ** for $p < 0.01$; N.S.: Not significant.

the molecular organization of hMSCs under high viscosity stimulation. To achieve this, we analyzed the expressions and distribution patterns of focal adhesion proteins, specifically paxillin, along with actin filaments through immunofluorescence staining (Fig. 2A). In comparison with hMSCs in cultured medium (DMEM), hMSCs in higher viscosity medium (21.83 and 68.14 cP) for 1 h displayed a larger number of paxillin-marked FAs (Fig. 2B) and also induced the formation of more actin stress fibers. These fibers included dorsal stress fibers, linked to focal adhesions at their distal ends along the cell periphery, and ventral stress fibers, attached to focal adhesions at both ends (Fig. 2C). We further examined actin stress formation dynamics in hMSCs during cell spreading under high-viscosity conditions. To visualize F-actin structures, we transfected hMSCs with Lifeact-GFP. Time-lapse images capturing both cell spreading and F-actin formation were acquired via integrated fluorescence microscopy and interference reflection microscopy (Supplementary Movie 3). Our results revealed a significant increase in formation of actin stress fibers, accompanied by enhanced cell spreading, in rapid response to high-viscosity stimulation (Fig. S2). These findings underscore the pivotal role of viscosity in promptly influencing cytoskeletal dynamics and cellular morphology.

To investigate whether the sustained exposure to high viscosity consistently promotes the maturation of focal adhesions over an extended period, we applied interference reflection microscopy (IRM) and fluorescence time-lapse imaging microscopy of hMSCs transfected with paxillin-GFP. This allowed us to observe cell spreading and paxillin dynamics in response to the high-viscosity medium (68.14 cP) over a 6-h period (Supplementary Movie 4 & Fig. S1 D). These images vividly illustrated that the high viscosity medium continuously enhances focal

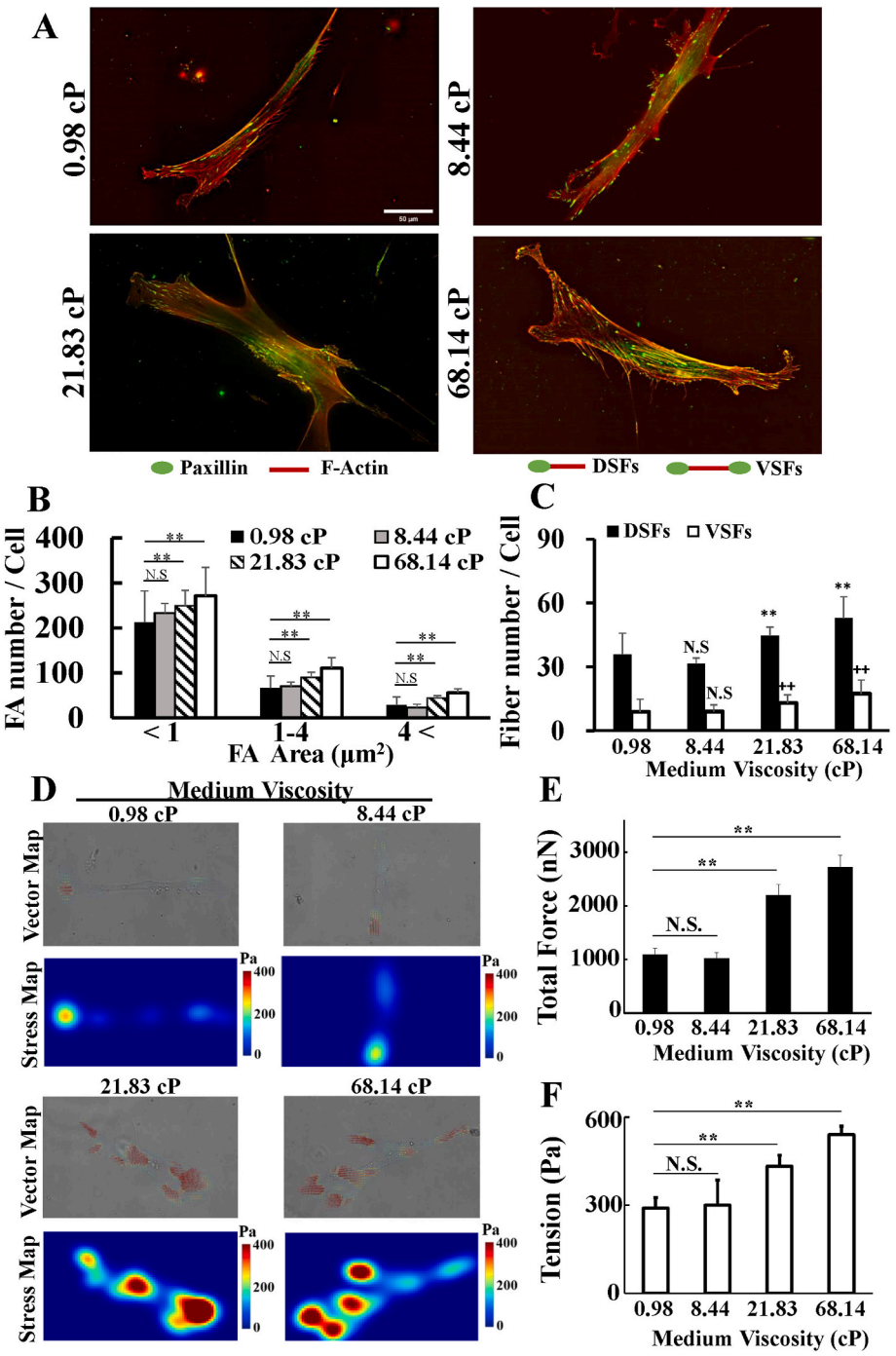


**Fig. 2.** Medium with higher viscosity promoted actin polymerization and focal adhesion maturation of human mesenchymal stem cells (hMSCs) to elevate intracellular tension. (A) Representative immunofluorescence micrographs of hMSCs cultured in DMEM with viscosities of 0.98 cP, 8.44 cP, 21.83 cP, and 68.14 cP for 1 h; red: TRITC-labeled phalloidin for actin, and green: FITC-labeled paxillin. Scale bars = 50 μm. **(B–C)** hMSCs cultured in a high-viscosity medium (21.83 & 68.14 cP) for 1 h displayed a larger number of focal adhesions and actin stress fibers, including both Dorsal and Ventral stress fibers (DSFs & VSFs). Data represent mean ± SD (n = 10). Significant differences from "DSFs of hMSCs" are indicated by **P < 0.001, and from "DSFs" by++ P < 0.001 in Figure C. **(D–F)** Elevated viscosity induced cells to generate stronger cell traction forces and intracellular tension after 1 h. Data represent mean ± SD (n = 15). *for p < 0.05 and ** for p < 0.01; N.S.: Not significant. (For interpretation of the references to color in this figure legend, the reader is referred to the Web version of this article.)

adhesion maturation over an extended period. Furthermore, we analyzed the organization of focal adhesions and stress fibers of hMSCs cultured in low (0.98 cP) and high (68.14 cP) viscosity of differentiation medium at day 1, 3, and 7. These results revealed that high viscosity medium sustainably enhance cell adhesion, actin stress fibers, and spreading area of hMSCs over an extended period (Fig. S3). Taken together, these results suggest a sustained enhancement of spreading area and formation of actin stress fibers and focal adhesion over an extended duration in the presence of the viscous medium.

Supplementary data related to this article can be found online at https://doi.org/10.1016/j.mtbio.2024.101058

### 3.3. hMSCs displayed high intracellular tension to counter-balance stronger viscous forces

Previous studies have established that when subjected to physical

force stimulation, cells adjust their traction forces and intracellular tension by remodeling the cytoskeleton and focal adhesion complexes to balance extracellular and intracellular forces [62–64]. We hypothesize that the changes in hMSCs are attributed to alterations in intracellular tension to counter-balance the effects of viscosity stimulation. To test this hypothesis, we applied traction force microscopy to quantify the traction forces exerted by hMSCs in response to four different medium viscosities. Subsequently, we calculated their intracellular tension (Fig. 2D). Our results indicated that hMSCs exhibited stronger traction forces and intracellular tension, correlated with the high expression of large focal adhesion-associated proteins and actin stress fibers in response to elevated viscosity stimulation for 1hr (Fig. 2E and F). Furthermore, in the medium with higher viscosity (21.83 cP and 68.14 cP), cells exerted stronger traction forces not only at both ends but also in regions such as lamellipodia and the central cell region, correlated with the locations of ventral stress fiber and dorsal stress fiber formation (Fig. 2A and D). In summary, when hMSCs were subjected to high viscosity stimulation, they adjusted their biomechanical properties to counteract the viscous force by promoting the maturation of focal adhesions and the formation of stress fibers, leading to stronger traction forces, larger cell spreading area, and elevated intracellular tension. Together, these mechanisms worked to balance the viscous force on the cell membrane.

### 3.4. Higher viscosity of extracellular fluid stimulated and promoted osteogenic lineage

Next, we investigated whether the changes in hMSC mechanical properties, induced by viscosity, could promote osteogenic lineage. To evaluate the impact of extracellular fluid viscosity on hMSC differentiation, we prepared four different viscosities (0.98, 8.44, 21.83, and 68.14 cP) of differentiation medium (DM), each comprising a 1:1 combination of adipogenesis and osteogenesis induction medium, and exposed hMSCs to these four distinct viscosity levels of DM for 14 days. We then quantified the proportions of cells exhibiting alkaline phosphatase (ALP) activity, an indicator of osteogenesis, and those containing lipid droplets, indicative of adipogenesis, to assess how viscosity affects hMSC commitment (Fig. 3A). Our findings demonstrated that higher viscosity (21.83 cP and 68.14 cP) promoted osteogenic lineage in hMSCs while concurrently suppressing adipogenesis when compared to those cultured in lower viscosity (0.98 and 8.44 cP) differentiation medium (Fig. 3B).

### 3.5. Higher viscosity of extracellular fluid activated TRPV4 to boost cell spreading and promote osteogenesis

In the context of hMSCs, TRPV4 plays a significant role in sensing shear stress [65] and hypo-osmotic pressure [66], thereby enhancing the osteogenic differentiation process. However, it remained uncertain whether TRPV4 could be activated by viscosity-related stimulation to regulate the mechanical properties of hMSCs, and to subsequently enhance osteogenic differentiation. To investigate whether ECF viscosity triggers calcium influx in hMSCs through the activation of TRPV4, we incubated hMSCs with the fluorescent calcium indicator (Fluo-8 am) and examined them via an integrated fluorescence microscopy and interference reflection microscopy platform. This approach enabled us to simultaneously visualize and quantify intracellular calcium levels and cell spreading.

Additionally, we used the TRPV4 antagonist (GSK205) to further validate the involvement of TRPV4 in this process. We observed a substantial increase in intracellular calcium levels concomitant with an expansion in cell area when the culture medium (0.98 cP) was swiftly switched to a high viscosity state (68.14 cP). Notably, when hMSCs were pre-treated with a 10 μM of GSK205 for 3 h prior to viscosity stimulation, we observed a reduction in both calcium influx and cell area compared to hMSCs without GSK205 pretreatment (Fig. 4A and B and

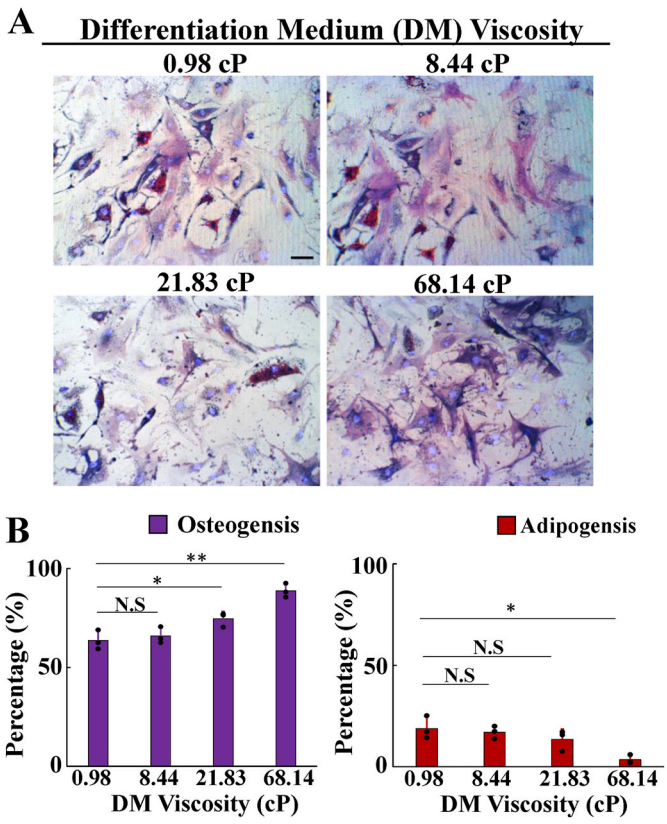


**Fig. 3.** Elevated viscosity promoted early osteogenesis in human mesenchymal stem cells (hMSCs). (A) Representative micrographs of mesenchymal stem cells (hMSCs) cultured in differentiation medium with varying viscosities for 14 days. The cells were then stained to visualize the presence of ALP activity (in purple) and lipids (Oil Red O, red). Scale bars = 50 μm. **(B)** The percentage of osteogenesis (ALP-positive cells) and adipogenesis (Oil Red O-positive cells) in hMSCs, as depicted in (A). Data represent mean ± SD (n = 3; i.e., three replicated independent experiments). * for $p < 0.05$ and ** for $p < 0.01$. ; N.S.: Not significant. (For interpretation of the references to color in this figure legend, the reader is referred to the Web version of this article.)

Supplementary Movie 5). This suggests that TRPV4 activation plays a crucial role in mediating the response of hMSCs to viscosity-induced mechanical stimulation, including the increased calcium influx and cell spreading.

To further validate the translocation of TRPV4 to the cell membrane induced by ECF viscosity, we quantified TRPV4 expression on the cell membrane using surface immunostaining on non-permeabilized fixed hMSCs. Our results indicated that, compared to hMSCs cultured in a regular medium, high viscosity led to a larger amount of TRPV4 on the cell membrane of hMSCs (Fig. 4C–F). In contrast, in high viscosity stimulation, the translocation of TRPV4 to the membrane was suppressed by pretreatment with 10 μM of GSK205. Furthermore, we observed that viscosity-enhanced osteogenic lineage was also suppressed by TRPV4 antagonist (Fig. 4G–J). These findings collectively demonstrated the translocation of TRPV4 to the hMSCs' membrane, in response to activated calcium influx due to viscosity stimulation. This activation, in turn, enhanced cell mechanical properties and promoted osteogenic lineage.

Supplementary data related to this article can be found online at https://doi.org/10.1016/j.mtbio.2024.101058

### 3.6. Calcium influx, induced by higher viscosity of extracellular fluid, promoted the nuclear translocation of NFATc1

NFATc1(nuclear factor of activated T cells 1) is another vital

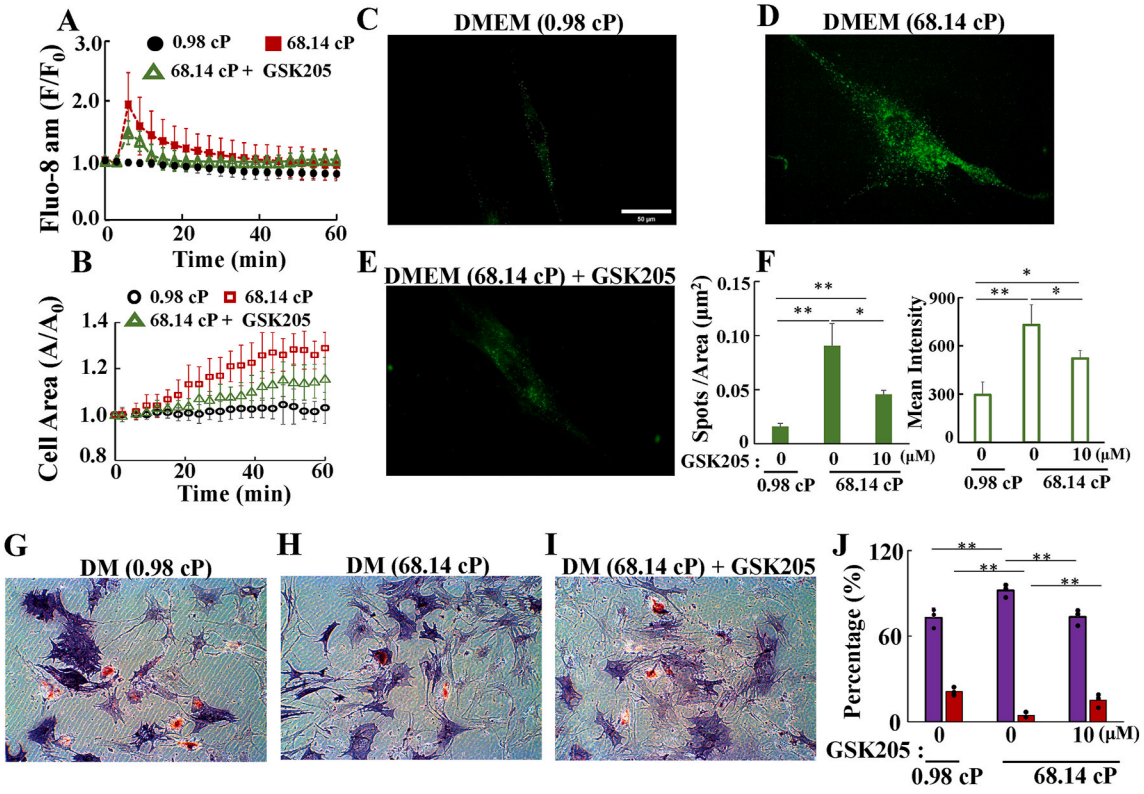


**Fig. 4.** Higher extracellular viscosity enhanced the translocation of TRPV4 to the cell membrane, thereby promoting calcium influx and osteogenic lineage in hMSCs. **(A)** The time course of intracellular $Ca^{2+}$ levels, quantified in terms of Fluo 8-am, in hMSCs with and without a 3-h pre-treatment of the 10 μM TRPV4 inhibitor (GSK205), followed by stimulation with a high-viscosity medium (68.14 cP). Cell culture in DMEM (0.98 cP) serves as control. **(B)** Time-dependent relative changes in hMSCs' area, corresponding to Fig. 4A. Data represent mean ± SD (n = 10). **(C–E)** The surface labeling of TRPV4 (in green) on hMSCs, with and without prior treatment with 10 μM of GSK205 (a TRPV4 antagonist), followed by stimulation with a highly viscous medium (68.14 cP) for 1 h. The surface labeling procedure included the blocking of non-permeabilized fixed hMSCs with BSA for 1 h, followed by a 1-h incubation with anti-TRPV4 and two PBS washes. Finally, the cells were incubated with an Alexa Fluor 488-conjugated antibody for 1 h. Scale bars = 50 μm. **(F)** Quantification of the number and the intensity of TRPV4 fluorescence spots on the cell membrane, as depicted in (C–E). Data represent mean ± SD (n = 15). **(G–I)** Representative micrographs of hMSCs, cultured in differentiation medium with and without treatment with 10 μM of GSK205 followed by stimulation with a highly viscous medium (68.14 cP) for 14 days. The cells were stained to visualize the presence of ALP activity (in purple) and lipids (Oil Red O, red). Scale bars = 50 μm. **(J)** The percentage of osteogenesis (ALP-positive cells) and adipogenesis (Oil Red O-positive cells) in hMSCs, as depicted in (I). Data represent mean ± SD (n = 3; i.e., three replicated independent experiments). * for $p < 0.05$ and ** for $p < 0.01$. ; N.S.: Not significant. (For interpretation of the references to color in this figure legend, the reader is referred to the Web version of this article.)

transcription factor in osteogenic differentiation, activated by calcium signaling pathways [67,68]. To further substantiate the notion that calcium influx, facilitated by mechanisms such as TRPV4 activation in response to viscosity stimulation, is pivotal in enhancing osteogenic lineage, we used immunostaining to assess the distribution of NFATc1 in hMSCs subjected to high-viscosity stimulation (68.14 cP) (Fig. 5A). Our findings revealed an elevation in the translocation of NFATc1 into the nucleus after exposure to high viscosity (68.14 cP) for 1 h, associated with increased membrane translocation of TRPV4 and enhanced cell spreading (Fig. 5B–D). When we pretreated hMSCs with a 10 μM of GSK205 and subsequently subjected them to high-viscosity medium stimulation (68.14 cP), we observed a reduced translocation of NFATc1 into the nucleus, concomitant with a decreased expression of TRPV4 on the cell membrane, and a decrease in cell area (Fig. 5B–D).

### *3.7. Higher viscosity of extracellular fluid induced nuclear deformation and nuclear translocation of YAP*

Based on our research findings, which demonstrated that a high-viscosity medium can enhance cell spreading area and increase traction force, we sought to investigate whether elevated viscosity induces nuclear deformation and promotes YAP nuclear translocation. To accomplish this, we used confocal microscopy to track the 3D nuclear morphology of live hMSCs before and after exposure to the high-viscosity medium *(68.14 cP)*. We observed that higher viscosity led to an expansion of the maximum projected nuclear area, a reduction in maximum nuclear thickness, and a decrease in nuclear volume, and ultimately resulting in nuclear flattening and compression (Fig. 6A and B). Furthermore, immunostaining of YAP and the nucleus in hMSCs cultured in media both without and with the addition of a high-viscosity supplement (Fig. 6C and D) revealed that compared to those cultured in a lower-viscosity medium, cells cultured in higher-viscosity medium exhibited a significant increase in YAP nuclear localization.

## 4. Discussion

Bone marrow is a viscous tissue with viscosity ranging from 37.5 to 400 cP; it resides in the bones and houses MSCs [25]. MSCs play a crucial role in bone regeneration as they differentiate into osteoblasts. MSCs are uniquely exposed to various mechanical stimuli in the bones. These stimuli include hydrostatic pressure, fluid-induced shear stress, topographical cues, stiffness, and viscosity, all of which have a significant impact on functionality of MSCs [25]. In this study, we demonstrated that a medium with a viscosity in the range of 21.83–68.14 cP, closely resembling the physiological viscosity of bone marrow, can promote osteogenic lineage while suppressing adipogenic differentiation. Kyubae Lee et al. reported their study where they cultured hMSCs in 3D gelatin solutions with varying viscosities to explore how gelatin viscosity affects

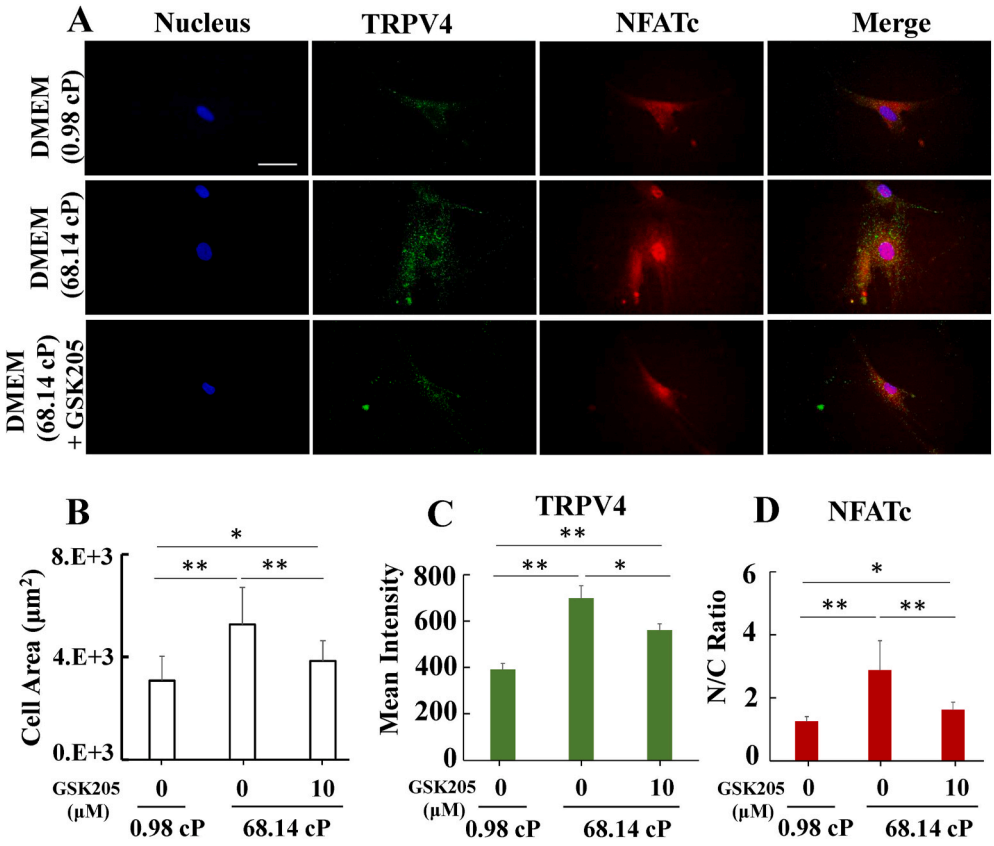


**Fig. 5.** Higher extracellular viscosity promoted membrane translocation of TRPV4 and the nuclear translocation of NFATc1. (A) Immunofluorescence micrographs displaying NFATc (in red), TRPV4 on membrane (in green), and the nucleus (in blue), in hMSCs with and without prior treatment with GSK205 (10 μM), and subsequently stimulated with a highly viscous medium (68.14 cP) for 1 h. Scale bars = 50 μm. **(B)** Cell area, **(C)** mean fluorescence intensity of TRPV4, and **(D)** the ratio of NFATc in the nucleus to that in the cytoplasm of hMSC, as indicated in (A). Data represent mean ± SD (n = 15). * for $p < 0.05$ and ** for $p < 0.01$. (For interpretation of the references to color in this figure legend, the reader is referred to the Web version of this article.)

MSCs' osteogenesis and adipogenesis [48]. Consistently, their findings revealed that a high-viscosity gelatin solution enhances the activation of osteogenesis-related genes, such as ALP and Runx2, and promotes osteogenic differentiation. However, the mechanisms underlying how hMSCs sense and respond to viscosity stimulation to ultimately enhance osteogenic differentiation remain unclear. Here, we observed that high viscosity medium prompted early differentiation of hMSCs towards an osteogenic pathway. This effect was mediated through the activation of TRPV4, which triggered calcium influx and the translocation of NFATc into the nucleus, and ultimately leading to the up-regulation of osteogenesis-related genes, ALP.

TRPV4, a calcium-permeable membrane ion channel, plays a crucial role in bone development. In human, mutations in the TRPV4 gene have been linked to disruptions in normal skeletal development [69]. The reduced osteogenic differentiation potential observed in mesenchymal stem cells (MSCs) from TRPV4 knockout mice underscores the significance of TRPV4 in processes related to bone formation [70]. Moreover, TRPV4-initiated mechano-regulatory pathways are pivotal in guiding skeletal development. Consequently, TRPV4 represents a valuable target for advancing strategies aimed at skeletal regeneration and repair [71]. Additionally, TRPV4 can be directly activated by membrane tension or strain induced by shear flow, hypo-osmotic pressure, and viscous mediums, leading to enhanced calcium influx [23,66,72]. Consequently, mechanically activated TRPV4 has been widely applied to promote osteogenic differentiation of MSCs. Previous research has revealed that fluid shear stress [65] and hypo-osmotic pressure [66] can potentially boost osteogenesis, indicating that these mechanical factors might induce osteogenic differentiation through the TRPV4 signaling pathway. In this study, we delved into the mechanisms underlying how viscosity-induced enhancements in cell spreading, intracellular tension, and nuclear deformation are regulated by the activation of TRPV4-mediated calcium influx. This interplay between TRPV4 activation, elevated calcium levels, and biomechanical changes facilitates the nuclear translocation of NFATc and YAP, ultimately promotes osteogenic differentiation. To further confirm the role of a high-viscosity medium in enhancing the mechanical properties of hMSCs and promoting osteogenic lineage, we prepared another high-viscosity medium by adding 1 % poly (ethylene oxide) (PEO) to the cultured medium, which increased the medium's viscosity to 160 cP [24]. Consistently, we observed that the 1 % PEO-enriched medium led to increments in cell spreading, cell traction forces, intracellular tension, and calcium influx (Figs. S4A–D). Furthermore, the enhanced calcium influx and intracellular tension facilitated the translocation of NFATc and YAP into the nucleus, respectively (Fig. S4 E-H), ultimately promoted osteogenic lineage (Figs. S4I–J).

Macromolecular crowding (MMC), a crucial element within cellular environments defined by the dense arrangement of biomolecules, leads to the excluded volume effect (EVE) [73–75]. This phenomenon significantly influences many cellular processes, encompassing protein phase separation [76], tissue engineering [77], extracellular matrix organization [78,79], and differentiation [80]. MMC amplifies the extracellular accumulation of human bone marrow-derived mesenchymal stem cells, indicating its pivotal involvement in tissue regeneration [78]. Furthermore, within the realm of adipogenic differentiation, adding MMC to culture media fosters adipogenic differentiation in stem cells, highlighting its regulatory role in steering cellular fate determinations [80]. To elucidate whether the observed increase in cell adhesion and spreading with 0.8 % methylcellulose medium is attributed to viscosity,

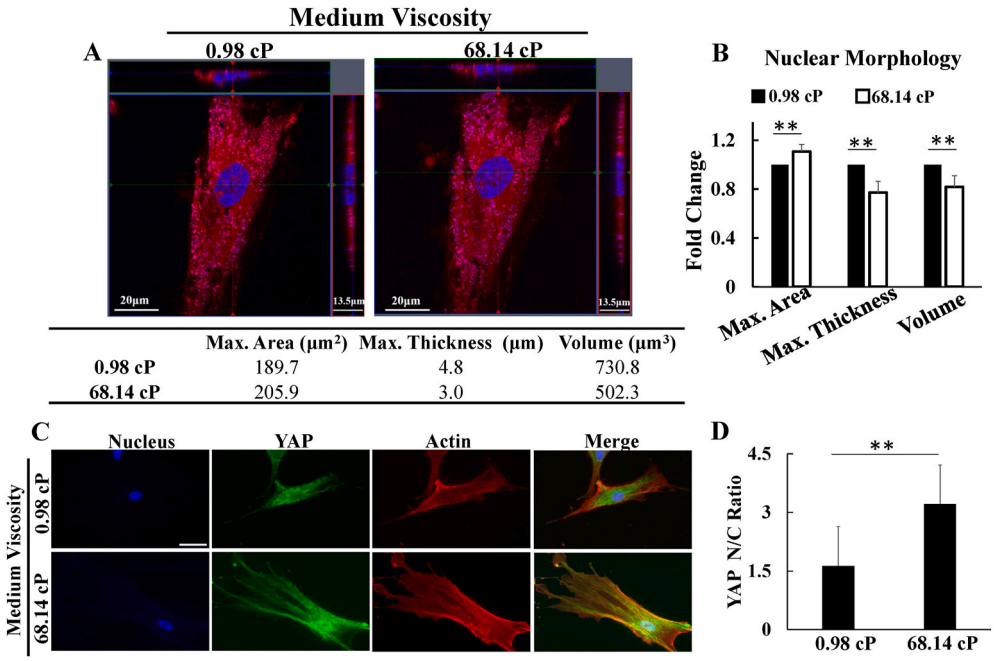


| | Max. Area (μm²) | Max. Thickness (μm) | Volume (μm³) |
|---|---|---|---|
| 0.98 cP | 189.7 | 4.8 | 730.8 |
| 68.14 cP | 205.9 | 3.0 | 502.3 |

**Fig. 6.** An increase in viscosity flattened and compressed the nucleus, leading to the translocation of YAP into the nucleus. (A) Upper**:** Representative orthogonal projections of 3D nuclear morphology of a living hMSC before and after exposure to a high-viscosity medium (68.14 cP). Blue: hochest 3342 staining for the nucleus. Red: celltracker red staining for the cytoplasm. Lower: Quantitative analysis of nuclear morphology parameters, including maximum projected nuclear area, maximum nuclear thickness, and volume, before and after exposure to high viscosity medium (68.14 cP). **(B)** Fold changes in nuclear morphology upon transitioning to a high-viscosity medium (68.14 cP). Data represent mean ± SD (n = 10). **(C)** Immunofluorescence micrographs displaying nucleus (in blue), YAP (in green), and the actin (in red) of hMSCs in the medium with viscosities of 0.98 cP and 68.14 cP. Scale bars = 50 μm. **(D)** The ratio of YAP in the nucleus to that in the cytoplasm of hMSCs, as indicated in (C). Data represent mean ± SD (n = 15). * for $p < 0.05$ and ** for $p < 0.01$. (For interpretation of the references to color in this figure legend, the reader is referred to the Web version of this article.)

MMC induction, or a combination of both, we prepared two MMC-inducing agents, 0.6 % w/v Dextran (Mw: 70 kDa) and 3.6 % w/v Ficoll400 (Mw: 400 kDa) in culture medium (DMEM supplemented with 10 % FPS and 1 % P/S), with similar molarity (90.9 μM) to 0.8 % w/v MC, and assessed their viscosity. We found that the viscosity of 0.6 % w/v Dextran (1.20 ± 0.01 cP) and 3.6 % w/v Ficoll400 (1.68 ± 0.01 cP) were comparable to that of the culture medium (0.98 ± 0.04 cP) (Fig. S5A). We quantified their osmolality via an osmometer (WESCOR Vapro 5520). The osmolality of 0.6 % Dextran (311 ± 0.0 mmol/kg) and 3.6 % Ficoll400 (318.3 ± 3.4 mmol/kg) were slightly higher compared to that of the culture medium (286.3 ± 0.9 mmol/kg) (Fig. S5A); yet, they did not exceed the threshold for significant hyperosmolarity (320 mmol/kg) [81]. Consistently, time-lapse interference reflection microscopy (IRM) imaging of hMSCs exposed to low viscosity of 0.6 % Dextran and 3.6 % Ficoll400, revealed no significant alteration in cell spreading area (Supplementary Movie 5 and Fig. S5 B-C). Subsequently, we examined the impact of a high concentration of 10 % (252 μM) and 20 % w/v (505 μM) Ficoll400, a commonly employed concentration for MMC. We found that the viscosity slightly increased in 10 % Ficoll400 (3.50 ± 0.02 cP) and significantly heightened in 20 % Ficoll400 (15.04 ± 0.13 cP). Moreover, 10 % (334.7 ± 3.8 mmol/kg) and 20 % (382.7 ± 4.6 mmol/kg) Ficoll400 resulted in significant hyperosmolarity (≥320 mmol/kg) and severe hyperosmolarity (≥350 mmol/kg) [81], respectively (Fig. S5A). Interestingly, high concentration of Ficoll400 medium caused cell retraction with decreased cell area (Supplementary Movie 6 & Figs. S5B–C), possibly attributable to either the MMC itself or its hyperosmolar effect. These results suggest that the augmented cell spreading observed with 0.8 % methylcellulose medium (68.14 ± 1.59 cP) is likely due to viscosity rather than MMC induction. However, further investigations may be warranted to fully elucidate the interplay between viscosity and MMC in influencing cellular behavior.

Supplementary data related to this article can be found online at https://doi.org/10.1016/j.mtbio.2024.101058

## 5. Conclusions

In summary, our findings revealed that medium viscosity is pivotal in promoting osteogenic lineage in hMSCs through a series of interconnected mechanisms. This process begins with the activation of TRPV4 channels, which triggers their translocation to the cell membrane and the subsequent calcium influx. This sequence of events leads to the increments of cell spreading and intracellular tension, characterized by the formation of robust actin stress fibers and mature focal adhesions. These changes ultimately drive the translocation of NFATc and YAP into the nucleus and further enhance pre-osteogenic activity for osteogenic differentiation (Fig. 7). Tuning cell culture medium viscosity could be a viable and flexible approach to achieve synergistic and more efficient hMSC differentiation towards the osteogenic path.

## Funding

This work was supported by grants from the Ministry of Education, Higher Education SPROUT Project for Cancer Progression Research Center (111W31101), the Cancer and Immunology Research Center (112W31101 &113W031101), and the National Science and Technology Council. (NSTC 112-2740-B-A49 -001, NSTC 111-2740-B-A49 -001 & NSTC 112-2221-E-A49 -128-).

## CRediT authorship contribution statement

**Yin-Quan Chen:** Writing – review & editing, Writing – original draft, Visualization, Supervision, Methodology, Funding acquisition, Conceptualization. **Ming-Chung Wu:** Methodology, Investigation. **Ming-Tzo Wei:** Writing – review & editing, Visualization. **Jean-Cheng Kuo:** Writing – review & editing, Visualization, Resources, Methodology. **Helen Wenshin Yu:** Software, Resources, Methodology. **Arthur Chiou:** Writing – review & editing, Investigation.

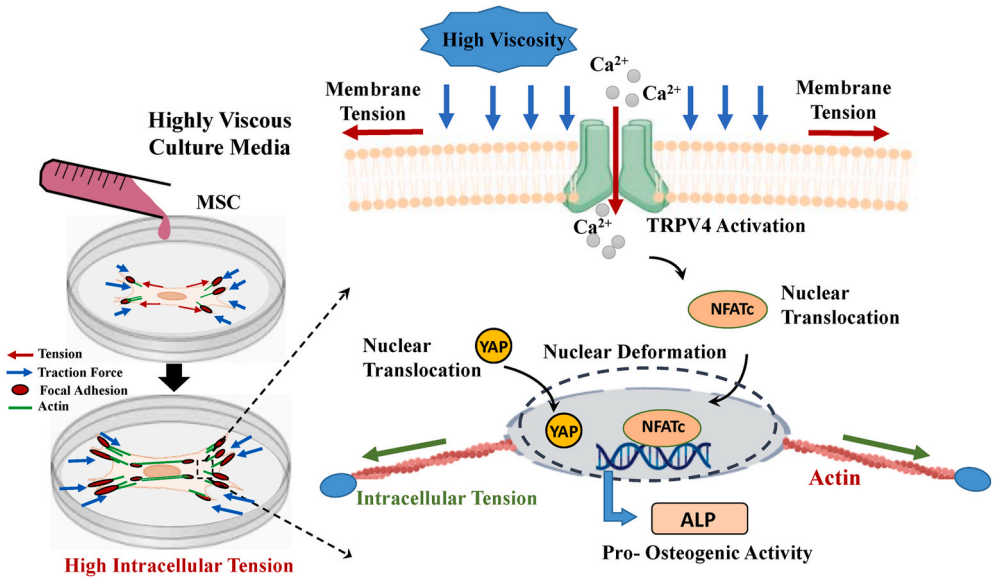


**Fig. 7.** A schematic diagram illustrating the proposed model to highlight the influence of high extracellular fluid viscosity on the biomechanical and biochemical properties of hMSCs to promotedifferentiation towards the osteogenic path.

## Declaration of competing interest

The authors declare that they have no known competing financial interests or personal relationships that could have appeared to influence the work reported in this paper.

## Data availability

Data will be made available on request.

## Acknowledgements

We gratefully acknowledge the technical services from the National Genomics Center for Clinical and Biotechnological Applications of the Cancer Progression Research Center (National Yang Ming Chiao Tung University), and the National Core Facility for Biopharmaceuticals (NCFB).

## Appendix A. Supplementary data

Supplementary data to this article can be found online at https://doi.org/10.1016/j.mtbio.2024.101058.

## References

[1] B. Arjmand, M. Sarvari, S. Alavi-Moghadam, M. Payab, P. Goodarzi, K. Gilany, N. Mehrdad, B. Larijani, Prospect of stem cell therapy and regenerative medicine in osteoporosis, Front. Endocrinol. 11 (2020) 430.
[2] Y. Jiang, P. Zhang, X. Zhang, L. Lv, Y. Zhou, Advances in mesenchymal stem cell transplantation for the treatment of osteoporosis, Cell Prolif. 4 (1) (2021) e12956.
[3] L. Hu, C. Yin, F. Zhao, A. Ali, J. Ma, A. Qian, Mesenchymal stem cells: cell fate decision to osteoblast or adipocyte and application in osteoporosis treatment, Int. J. Mol. Sci. 19 (2) (2018) 360.
[4] F. Shang, Y. Yu, S. Liu, L. Ming, Y. Zhang, Z. Zhou, J. Zhao, Y. Jin, Advancing application of mesenchymal stem cell-based bone tissue regeneration, Bioact. Mater. 6 (3) (2021) 666–683.
[5] J. Petzold, E. Gentleman, Intrinsic mechanical cues and their impact on stem cells and embryogenesis, Front. Cell Dev. Biol. 9 (2021) 761871.
[6] M. van Griensven, S. Diederichs, S. Roeker, S. Boehm, A. Peterbauer, S. Wolbank, D. Riechers, F. Stahl, C. Kasper, Mechanical strain using 2D and 3D bioreactors induces osteogenesis: implications for bone tissue engineering, Adv. Biochem. Eng. Biotechnol. 112 (2009) 95–123.
[7] K.H. Vining, D. Mooney, Mechanical forces direct stem cell behaviour in development and regeneration, Nat. Rev. Mol. Cell Biol. 18 (12) (2017) 728–742.
[8] N. Xie, C. Xiao, Q. Shu, B. Cheng, Z. Wang, R. Xue, Z. Wen, J. Wang, H. Shi, D. Fan, Cell response to mechanical microenvironment cues via Rho signaling: from mechanobiology to mechanomedicine, Acta Biomater. 15 (2023) 1–20.
[9] D.A. Fletcher, R.D. Mullins, Cell mechanics and the cytoskeleton, Nature 463 (7280) (2010) 485–492.
[10] D.H. Kim, P.K. Wong, J. Park, A. Levchenko, Y. Sun, Microengineered platforms for cell mechanobiology, Annu. Rev. Biomed. Eng. 11 (2009) 203–233.
[11] M.L. Rodriguez, P.J. McGarry, N. Sniadecki, Review on cell mechanics: experimental and modeling approaches, Appl. Mech. Rev. 65 (6) (2013) 060801.
[12] M.M. Moghaddam, S. Bonakdar, M.R. Shariatpanahi, M.A. Shokrgozar, S. Faghihi, The effect of physical cues on the stem cell differentiation, Curr. Stem Cell Res. Ther. 14 (3) (2019) 268–277.
[13] A.J. Engler, S. Sen, H.L. Sweeney, D.E. Discher, Matrix elasticity directs stem cell lineage specification, Cell Death Dis. 126 (4) (2006) 677–689.
[14] S.K. Dash, V. Sharma, R.S. Verma, S. Das, Low intermittent flow promotes rat mesenchymal stem cell differentiation in logarithmic fluid shear device, Biomicrofluidics 14 (5) (2020) 054107.
[15] D. Zhang, R. Zhang, X. Song, K.C. Yan, H. Liang, Uniaxial cyclic stretching promotes chromatin accessibility of gene loci associated with mesenchymal stem cells morphogenesis and osteogenesis, Front. Cell Dev. Biol. 9 (2021) 664545.
[16] J. Lee, A.A. Abdeen, T.H. Huang, K. Kilian, Controlling cell geometry on substrates of variable stiffness can tune the degree of osteogenesis in human mesenchymal stem cells, J. Mech. Behav. Biomed. Mater. 38 (2014) 209–218.
[17] R.S. Rosenson, A.U. Mccormick, F. Eugene, Distribution of blood viscosity values and biochemical correlates in healthy adults, Clin. Chem. 42 (8) (1996) 1189–1195.
[18] J. Gonzalez-Molina, X. Zhang, M. Borghesan, J.M. Silva, M. Awan, B. Fuller, N. Gavara, C. Selden, Extracellular fluid viscosity enhances liver cancer cell mechanosensing and migration, Biomaterials 177 (2018) 113–124.
[19] T. Furubayashi, D. Inoue, A. Kamaguchi, Y. Higashi, T. Sakane, Influence of formulation viscosity on drug absorption following nasal application in rats, Drug Metab, Pharmacok 22 (3) (2007) 206–211.
[20] A. Cochis, L. Bonetti, R. Sorrentino, N. Contessi Negrini, F. Grassi, M. Leigheb, L. Rimondini, S. Farè, 3D printing of thermo-responsive methylcellulose hydrogels for cell-sheet engineering, Materials 11 (4) (2018) 579.
[21] D.W. Kufe, Mucins in cancer: function, prognosis and therapy, Nat. Rev. Cancer 9 (12) (2009) 874–885.
[22] T. Ahlfeld, V. Guduric, S. Duin, A.R. Akkineni, K. Schütz, D. Kilian, J. Emmermacher, N. Cubo-Mateo, S. Dani, M.v. Witzleben, J. Spangenberg, R. Abdelgaber, R.F. Richter, A. Lode, M. Gelinsky, Methylcellulose–a versatile printing material that enables biofabrication of tissue equivalents with high shape fidelity, Biomater. Sci. 8 (8) (2020) 2102–2110.
[23] K. Bera, A. Kiepas, I. Godet, Y. Li, P. Mehta, B. Ifemembi, C.D. Paul, A. Sen, S. A. Serra, K. Stoletov, J. Tao, G. Shatkin, S.J. Lee, Y. Zhang, A. Boen, P. Mistriotis, D. M. Gilkes, J.D. Lewis, C.M. Fan, A.P. Feinberg, M.A. Valverde, S.X. Sun, K. Konstantopoulos, Extracellular fluid viscosity enhances cell migration and cancer dissemination, Nature 611 (7935) (2022) 365–373.
[24] M. Pittman, E. Iu, K. Li, M. Wang, J. Chen, N. Taneja, M.H. Jo, S. Park, W.H. Jung, L. Liang, I. Barman, T. Ha, S. Gaitanaros, J. Liu, D. Burnette, S. Plotnikov, Y. Chen, Membrane ruffling is a mechanosensor of extracellular fluid viscosity, Nat. Phys. 18 (2022) 1112–1121.
[25] U.A. Gurkan, O. Akkus, The mechanical environment of bone marrow: a review, Biomed, Eng. 36 (2008) 1978–1991.

[26] S. Baratchi, J.G. Almazi, W. Darby, F.J. Tovar-Lopez, A. Mitchell, P. McIntyre, Shear stress mediates exocytosis of functional TRPV4 channels in endothelial cells, Cell. Mol. Life Sci. 73 (2016) 649–666.
[27] S.A. Mendoza, J. Fang, D.D. Gutterman, D.A. Wilcox, A.H. Bubolz, R. Li, M. Suzuki, D.X. Zhang, TRPV4-mediated endothelial Ca2+ influx and vasodilation in response to shear stress, Am. J. Physiol. Heart Circ. Physiol. 298 (2) (2010) H466–H476.
[28] V. Hartmannsgruber, W.T. Heyken, M. Kacik, A. Kaistha, I. Grgic, C. Harteneck, W. Liedtke, J. Hoyer, R. Köhler, Arterial response to shear stress critically depends on endothelial TRPV4 expression, PLoS One 2 (9) (2007) e827.
[29] L. Michalick, W.M. Kuebler, TRPV4—a missing link between mechanosensation and immunity, Front. Immunol. 11 (2020) 413.
[30] L.M. Grove, M.L. Mohan, S. Abraham, R.G. Scheraga, B.D. Southern, J.F. Crish, S. V. Naga Prasad, M. A Olman, Translocation of TRPV4-PI3Kγ complexes to the plasma membrane drives myofibroblast transdifferentiation, Sci. Signal. 12 (607) (2019) eaau1533.
[31] D.H. Kwon, F. Zhang, B.A. McCray, S. Feng, M. Kumar, J.M. Sullivan, W. Im, C. J. Sumner, S.Y. Lee, TRPV4-Rho GTPase complex structures reveal mechanisms of gating and disease, Nat. Commun. 14 (1) (2023) 3732.
[32] M. Lakk, D. Križaj, TRPV4-Rho signaling drives cytoskeletal and focal adhesion remodeling in trabecular meshwork cells, Am. J. Physiol. Cell Physiol. 320 (6) (2021) C1013–C1030.
[33] N. Wang, J.P. Butler, D.E. Ingber, Mechanotransduction across the cell surface and through the cytoskeleton, Science 260 (5111) (1993) 1124–1127.
[34] K. Ohashi, S. Fujiwara, K. Mizuno, Roles of the cytoskeleton, cell adhesion and rho signalling in mechanosensing and mechanotransduction, J. Biochem. 161 (3) (2017) 245–254.
[35] K.A. Jansen, D.M. Donato, H.E. Balcioglu, T. Schmidt, E.H. Danen, G. H. Koenderink, A guide to mechanobiology: where biology and physics meet, Biochim. Biophys. Acta 1853 (11) (2015) 3043–3052.
[36] F. Matsuoka, I. Takeuchi, H. Agata, H. Kagami, H. Shiono, Y. Kiyota, H. Honda, R. Kato, Morphology-based prediction of osteogenic differentiation potential of human mesenchymal stem cells, PLoS One 8 (2) (2013) e55082.
[37] X. Zhang, H. Zhao, Y. Li, D. Xia, L. Yang, Y. Ma, H. Li, The role of YAP/TAZ activity in cancer metabolic reprogramming, Mol. Cancer 17 (1) (2018) 1–10.
[38] S. Dupont, L. Morsut, M. Aragona, E. Enzo, S. Giulitti, M. Cordenonsi, F. Zanconato, J. Le Digabel, M. Forcato, S. Bicciato, N. Elvassore, S. Piccolo, Role of YAP/TAZ in mechanotransduction, Nature 474 (7350) (2011) 179–183.
[39] J.X. Pan, L. Xiong, K. Zhao, P. Zeng, B. Wang, F.L. Tang, D. Sun, H.H. Guo, X. Yang, S. Cui, W.F. Xia, L. Mei, W.C. Xiong, YAP promotes osteogenesis and suppresses adipogenic differentiation by regulating β-catenin signaling, Bone Res. 6 (1) (2018) 18.
[40] H. Nakajima, K. Yamamoto, S. Agarwala, K. Terai, H. Fukui, S. Fukuhara, K. Ando, T. Miyazaki, Y. Yokota, E. Schmelzer, H.G. Belting, M. Affolter, V. Lecaudey, N. Mochizuki, Flow-dependent endothelial YAP regulation contributes to vessel maintenance, Dev. Cell 40 (6) (2017) 523–536. e6.
[41] A. Elosegui-Artola, R. Oria, Y. Chen, A. Kosmalska, C. Pérez-González, N. Castro, C. Zhu, X. Trepat, P. Roca-Cusachs, Mechanical regulation of a molecular clutch defines force transmission and transduction in response to matrix rigidity, Nat. Cell Biol. 18 (5) (2016) 540–548.
[42] M.C. Wu, H.W. Yu, Y.Q. Chen, M.H. Ou, R. Serrano, G.L. Huang, Y.K. Wang, K. H. Lin, Y.J. Fan, C.C. Wu, J.C. Del Álamo, A. Chiou, S. Chien, J.C. Kuo, Early committed polarization of intracellular tension in response to cell shape determines the osteogenic differentiation of mesenchymal stromal cells, Acta Biomater. 163 (2023) 287–301.
[43] N. Koushki, A. Ghagre, L.K. Srivastava, C. Molter, A. Ehrlicher, Nuclear compression regulates YAP spatiotemporal fluctuations in living cells, Proc. Natl. Acad. Sci. U. S. A 120 (28) (2023) e2301285120.
[44] K.E. Scott, S.I. Fraley, P. Rangamani, A spatial model of YAP/TAZ signaling reveals how stiffness, dimensionality, and shape contribute to emergent outcomes, Proc. Natl. Acad. Sci. U. S. A 118 (20) (2021) e2021571118.
[45] R.D. González-Cruz, V.C. Fonseca, E. Darling, Cellular mechanical properties reflect the differentiation potential of adipose-derived mesenchymal stem cells, Proc. Natl. Acad. Sci. U. S. A 109 (24) (2012) E1523–E1529.
[46] R. McBeath, D.M. Pirone, C.M. Nelson, K. Bhadriraju, C. Chen, Cell shape, cytoskeletal tension, and RhoA regulate stem cell lineage commitment, Dev. Cell 6 (4) (2004) 483–495.
[47] K.A. Kilian, B. Bugarija, B.T. Lahn, M. Mrksich, Geometric cues for directing the differentiation of mesenchymal stem cells, Proc. Natl. Acad. Sci. U. S. A 107 (11) (2010) 4872–4877.
[48] K. Lee, Y. Chen, T. Yoshitomi, N. Kawazoe, Y. Yang, G. Chen, Osteogenic and adipogenic differentiation of mesenchymal stem cells in gelatin solutions of different viscosities, Adv. Healthcare Mater. 9 (23) (2020) 2000617.
[49] R. Cai, T. Nakamoto, T. Hoshiba, N. Kawazoe, G. Chen, Control of simultaneous osteogenic and adipogenic differentiation of mesenchymal stem cells, J, Stem Cell Res. Ther. 4 (8) (2014) 1000223.
[50] I.H. Huang, C.T. Hsiao, J.C. Wu, R.F. Shen, C.Y. Liu, Y.K. Wang, Y.C. Chen, C. M. Huang, J.C. Del Álamo, Z. Chang, GEF-H1 controls focal adhesion signaling that regulates mesenchymal stem cell lineage commitment, J. Cell Sci. 127 (19) (2014) 4186–4200.
[51] Y.Q. Chen, Y.S. Liu, Y.A. Liu, Y.C. Wu, J.C. Del Álamo, A. Chiou, O.K. Lee, Biochemical and physical characterizations of mesenchymal stromal cells along the time course of directed differentiation, Sci. Rep. 6 (1) (2016) 31547.
[52] S. Simmert, M.K. Abdosamadi, G. Hermsdorf, E. Schäffer, LED-based interference-reflection microscopy combined with optical tweezers for quantitative three-dimensional microtubule imaging, Opt Express 26 (11) (2018) 14499–14513.
[53] H. Verschueren, Interference reflection microscopy in cell biology: methodology and applications, J. Cell Sci. 75 (1985) 279–301.
[54] Y.L. Wang, R.J. Pelham Jr., Preparation of a flexible, porous polyacrylamide substrate for mechanical studies of cultured cells, Methods Enzymol. 298 (1998) 489–496.
[55] E. Stamhuis, W. Thielicke, PIVlab–towards user-friendly, affordable and accurate digital particle image velocimetry in MATLAB, J. Open Res. Software 2 (1) (2014) 30.
[56] D.T. Kovari, W. Wei, P. Chang, J.S. Toro, R.F. Beach, D. Chambers, K. Porter, D. Koo, J. E Curtis, Frustrated phagocytic spreading of J774A-1 macrophages ends in myosin II-dependent contraction, Biophys. J. 111 (12) (2016) 2698–2710.
[57] K.A. Beningo, Y.L. Wang, Flexible substrata for the detection of cellular traction forces, Trends, Cell Biol. 12 (2) (2002) 79–84.
[58] Y.Q. Chen, C.Y. Hung, M.T. Wei, J.C. Kuo, M.H. Yang, H.Y. Cheng, A. Chiou, Snail augments nuclear deformability to promote lymph node metastasis of head and neck squamous cell carcinoma, Front. Cell Dev. Biol. 10 (2022) 809738.
[59] C. Yeaman, K.K. Grindstaff, W.J. Nelson, New perspectives on mechanisms involved in generating epithelial cell polarity, Physiol. Rev. 79 (1) (1999) 73–98.
[60] T.D. Pollard, J. Cooper, Actin, a central player in cell shape and movement, Science 326 (5957) (2009) 1208–1212.
[61] M.A. Wozniak, K. Modzelewska, L. Kwong, P.J. Keely, Focal adhesion regulation of cell behavior, Biochim. Biophys. Acta 1692 (2–3) (2004) 103–119.
[62] H. Cirka, M. Monterosso, N. Diamantides, J. Favreau, Q. Wen, K. Billiar, Active traction force response to long-term cyclic stretch is dependent on cell pre-stress, Biophys. J. 110 (8) (2016) 1845–1857.
[63] X. Chen, Y. Li, M. Guo, B. Xu, Y. Ma, H. Zhu, X.Q. Feng, Polymerization force-regulated actin filament-Arp2/3 complex interaction dominates self-adaptive cell migrations, Proc. Natl. Acad. Sci. U. S. A 120 (2023) e2306512120.
[64] M.J. Paszek, N. Zahir, K.R. Johnson, J.N. Lakins, G.I. Rozenberg, A. Gefen, C. A. Reinhart-King, S.S. Margulies, M. Dembo, D. Boettiger, D.A. Hammer, V. M. Weaver, Tensional homeostasis and the malignant phenotype, Cancer Cell 8 (3) (2005) 241–254.
[65] K. Hu, H. Sun, B. Gui, C. Sui, TRPV4 functions in flow shear stress induced early osteogenic differentiation of human bone marrow mesenchymal stem cells, Biomed. Pharmacother. 91 (2017) 841–848.
[66] H.P. Lee, R. Stowers, O. Chaudhuri, Volume expansion and TRPV4 activation regulate stem cell fate in three-dimensional microenvironments, Nat. Commun. 10 (1) (2019) 529.
[67] P.G. Hogan, L. Chen, J. Nardone, A. Rao, Transcriptional regulation by calcium, calcineurin, and NFAT, Genes Dev. 17 (18) (2003) 2205–2232.
[68] J.W. Putney, Calcium signaling: deciphering the calcium–NFAT pathway, Curr. Biol. 22 (3) (2012) R87–R89.
[69] S.S. Kang, S.H. Shin, C.K. Auh, J. Chun, Human skeletal dysplasia caused by a constitutive activated transient receptor potential vanilloid 4 (TRPV4) cation channel mutation, Exp. Mol. Med. 44 (12) (2012) 707–722.
[70] C.J. O'conor, T.M. Griffin, W. Liedtke, F. Guilak, Increased susceptibility of Trpv4-deficient mice to obesity and obesity-induced osteoarthritis with very high-fat diet, Ann. Rheum. Dis. 72 (2) (2013) 300–304.
[71] N.S. Khatib, J. Monsen, S. Ahmed, Y. Huang, D.A. Hoey, N. Nowlan, Mechanoregulatory role of TRPV4 in prenatal skeletal development, Sci. Adv. 9 (4) (2023) eade2155.
[72] A.B. Veteto, D. Peana, M.D. Lambert, K.S. McDonald, T. Domeier, Transient receptor potential vanilloid-4 contributes to stretch-induced hypercontractility and time-dependent dysfunction in the aged heart, Cardiovasc. Res. 116 (11) (2020) 1887–1896.
[73] A.J. Boersma, B. Liu, B. Poolman, A sensor for quantification of macromolecular crowding in living cells, Nat. Methods 12 (2015) 227–229.
[74] I.M. Kuznetsova, K.K. Turoverov, V.N. Uversky, V.N. Uversky, What macromolecular crowding can do to a protein, Int. J. Mol. Sci. 15 (12) (2014) 23090–23140.
[75] C. Li, X. Zhang, M. Dong, X. Han, Progress on crowding effect in cell-like structures, Membranes 12 (6) (2022) 593.
[76] D. Cai, D. Feliciano, P. Dong, E. Flores, M. Gruebele, N. Porat-Shliom, S. Sukenik, Z. Liu, J. Lippincott-Schwartz, Phase separation of YAP reorganizes genome topology for long-term YAP target gene expression, Nat. Cell Biol. 21 (12) (2019) 1578–1589.
[77] A.D. Pieri, S.H. Korntner, H. Capella-Monsonis, D. Tsiapalis, S.V. Kostjuk, S. Churbanov, P. Timashev, A. Gorelov, Y. Rochev, D.I. Zeugolis, Macromolecular crowding transforms regenerative medicine by enabling the accelerated development of functional and truly three-dimensional cell assembled micro tissues, Biomaterials 287 (2022) 121674.
[78] A.S. Zeiger, F.C. Loe, R. Li, M. Raghunath, K.J. Van Vliet, Macromolecular crowding directs extracellular matrix organization and mesenchymal stem cell behavior, PLoS One 7 (5) (2012) e37904.
[79] C. Chen, F. Loe, A. Blocki, Y. Peng, M. Raghunath, Applying macromolecular crowding to enhance extracellular matrix deposition and its remodeling in vitro for tissue engineering and cell-based therapies, Adv. Drug Deliv. Rev. 63 (4–5) (2011) 277–290.
[80] X.M. Ang, M.H.C. Lee, A. Blocki, C. Chen, L.L.S. Ong, H.H. Asada, A. Sheppard, M. Raghunath, Macromolecular crowding amplifies adipogenesis of human bone marrow-derived mesenchymal stem cells by enhancing the pro-adipogenic microenvironment, Tissue Eng. Part A 20 (5–6) (2014) 966–981.
[81] S.A.B.B. Büyükkaragöz, Serum osmolality and hyperosmolar states, Pediatr. Nephrol. 38 (4) (2023) 1013–1025.